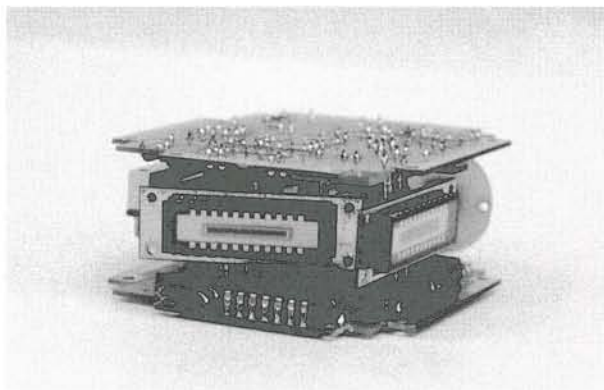


PSD – A useful component in space

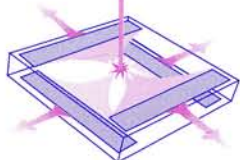
On a spacecraft in orbit around Earth, or flying into deep space, the Position Sensing Detector technology truly comes to its advantage. The mechanically simple and robust detector offers high reliability in the harsh space environment, with extreme temperatures, radiation of different kinds and high vibration levels when rocket engines are burning.



ASTRID 2 Sun sensor (with housing removed)

Almost every satellite, big, small or micro sized, carries one or several sun sensors, as one of the most important attitude control parameters is to know the sun location. There are mainly two types of sun sensors, Acquisition Phase Sun Sensors and Fine Pointing Sun Sensors. The first type has a very large field of view, with a limited accuracy. The primary use is to detect the sun directly after orbit injection, and make it possible for the attitude control system to turn the solar panels against the sun before the satellite runs out of battery power. It is also used during the flight as an emergency sensor if the satellite for a while loses the attitude control. The second type is used to fulfil more sophisticated pointing demands, when telescopes or other scientific instruments should point very accurately against distant objects. The pointing requirements can then be down to a few arc seconds.

ACR Electronic AB has in the past fifteen years designed and manufactured a number of sun sensors, the most recent types are: Two sun sensors on the successful Swedish satellite FREJA, launched 1992. One sensor was an Acquisition Phase Sun Sensor and the other a Fine Pointing Sun Sensor both were using a twodimensional SiTek PSD as sensor element. On the spinning micro satellite ASTRID 1, launched 1995, a different type of sun sensor was used to control the angle between spin axis and sun.



The sensor which covers almost the whole hemisphere uses two one-dimensional SITEK PSD:s. Two Fine Pointing Sun Sensors are qualified to be used on the next Swedish scientific satellite ODIN, planned to be launched 1998.

Finally, two Acquisition Phase Sun Sensors have been qualified for the next two micro satellites ASTRID 2 and ASTRID 3. ASTRID 2 will be launched early 1998 and ASTRID 3 has still no fixed launch date.

Beside the robustness of the PSD detector itself, it has also the advantage compared to one or two dimensional CCD:s, that the complexity of the supporting drive and readout electronics is significant reduced, which leads to smaller sensors with higher reliability. In particular, if the analog output signals can be used directly in a closed control loop, the component reduction is great.

The use of PSD:s on spacecrafts are of course not limited to sun sensors. The reliable components can have many other applications. One example is on ODIN, where a number of PSD:s are used in the main scientific instrument. They are to control the position of movable mirrors, which frequently shall return to a given position with high accuracy.

A more terrestrial application is the tracking sun sensors used on the high altitude balloon gondola PIROG. The sun sensor which contains 4 PSD:s tracks the sun automatically to an accuracy of a few arc seconds. It has flown and been recovered many times during ten years without any detector problems.



PIROG 8 Tracking sun sensor

Thermal Drift

In the course of the year we have built a new measuring system for the measurement of thermal drift - the parameter that is, perhaps, the most difficult one to measure.

When a PSD is subject to change in its temperature an alteration of the position signal is obtained despite there having taken place no actual change in the light's position. This is called thermal drift and is defined as the change of position on account of temperature change divided by the detector's length. SiTek is the only manufacturer that specifies this parameter.

For our standard components we measure this parameter in temperature intervals +20°C to +70°C within 80 % of the detector's length. Thermal drift for a one-dimensional SiTek PSD of 20 ppm/°C is typical. In practice this means that the total positional change for e.g. a 10 mm long PSD (1L10) in the case of a temperature change from +20°C to +70°C will be $20 \times 10^{-6} \times 10 \times 50 = 0,01$ mm which may affect the precision of the measurement. In normal temperature variations of a few degrees, however, the thermal drift in most cases is negligible.

It is important, however, to be aware that other parts too of the measurement system of which PSD is part are affected by temperature change. This applies, for example, to all the mechanical elements, in particular the mounting of PSD, lenses and light source as well as the electronics and light source.

This naturally applies, too, to our measuring system for the measurement of the component's thermal drift. Special attention must therefore be paid to the elimination of temperature change in other parts, in particular the mechanical mounting of PSD.

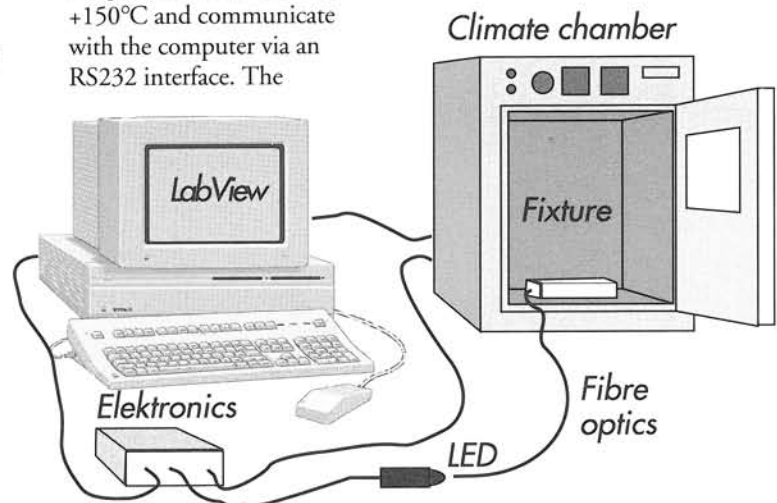
New measurement system

Our ten-year old measuring system is limited to measurements within the temperature range +20°C to +70°C. In addition, it was not able to handle all the newer components. We have now developed a new measurement system that handles measuring within the temperature range from -40°C to +85°C. The PSD is positioned on a measurement fixture inside a climate chamber. The light, which arrives via optical fibres, is adjusted to the right position on the component after

which the temperature is raised to the highest temperature of the measuring range. The signals from the PSD are read off and the position is calculated once every other degree, down to the lowest temperature of the measuring range. When this temperature is reached the total thermal drift is calculated.

Assembly

The measuring system comprises a climate chamber, a specially developed electronics, a fixture including fibre optics as well as an Apple Mac computer, see illustration. The measurement procedure with control and presentation of the result is programmed in the measurement program LabView. The climate chamber has an inner volume of 20 dm³, it can vary the temperature from -40°C to +150°C and communicate with the computer via an RS232 interface. The



electronics consists of a PSD amplifier, a driver for light diodes, demodulator, A/D converter as well as an RS232 interface for the computer. The fixtures that are different for each type of component are manufactured of ceramic. These fix the PSD on the fibre optics that supply the light for the components.

Dogs are my great interest

My name is Åsa Bengtsson, I am 26 years old and I started at SiTek in November. I form part of the production team. Having studied electronics-telecommunications at sixth-form level I have worked for a number of different companies including Volvo and Telia, at a district vet's and most recently at Triumfglass. The different jobs I have undertaken have been varied including motor car assembly, veterinary assistant and ice-cream manufacturing. This wide range of work is something I believe has been most useful as well as providing me with experience in different working environments. I am very fond of animals and I spend most of my spare time with my two dogs, either exercising them in the forest or training them at obedience classes. If they are not my own then there are others with which I assist in obedience training. I am very happy to start work at SiTek and it already feels as if I shall have a great time here.



Non-Contact in english only

We have had many positive responses to Non-Contact which has pleased us greatly and has convinced us that the newsletter meets a specific requirement. Now we wish to make it even better! For our Swedish readers this will represent a change - as from our next issue - in that we shall no longer produce a Swedish version. This may be viewed as a retrograde step but, on the other hand, we shall have more time and resources to develop Non-Contact in other respects. Equally, we are certain that English does not represent a barrier for our Swedish readers.

Contributions are welcome!

We also welcome all contributions to our newsletter from our readers - in particular, descriptions of different applications and areas of use of position-sensing detectors. We shall reward all published contributions with a beautiful fountain-pen.

Visit our website at
www.sitek.se

SiTek's PSD-school

Section 10 by Lars Stenberg ESDE AB

In section 9 we studied what happened when a collimated light beam strikes different types of surfaces and we found, on that occasion, that the simplest case - concerning the performance of a triangulation probe - is if the reflected surface gives rise to a large share of Lambert light dispersion. A triangulation probe also functions with Gaussian light dispersion but the smaller the beam angle of the Gaussian light dispersion the smaller the measurement area becomes.



Lars Stenberg

In order to understand the requirements we should make on the main lens, we shall now investigate how a light spot that strikes a surface is represented on the PSD detector's surface. Figure 1 shows the beam path in principle. From figure 1 it is evident that point A, corresponding to the measurement area's nearest position, is represented on point A' on the PSD detector. In the figure the points where B, C, D and N are represented are also plotted. With the aid of the formula

$$F''F' = \frac{\tan \beta}{\sin \gamma} (EF_{DE}'' + EF_{DE}')^2$$

that is presented in section 2 of the PSD school it is possible to calculate the distances C'B' and B'A' in figure 1. In this case, one should use the values for the detailed parameters that are stated in section 3 of the PSD school, namely: $\beta = 5,25^\circ$, $\gamma = 72,038^\circ$, $EF_{DE}'' = 41,380$ mm as well as $EF_{DE}' = 43,921$ mm. The result will then be that C'B' in figure 1 becomes = 3,9971 mm while B'A' = 4,2425 mm. The entire length of the detector F''F' = C'A' (in figure 1) = 8,24 mm.

It is also clear that the distance B'A' is a little longer than the distance C'B' in figure 1, to be more precise (4,2425 - 3,9971) mm = 0,2454 mm. In an analogous way the distance B'D' will also be somewhat longer than the distance E'B' in figure 1. If the spot DE, which is formed when the collimated light beam strikes the measurement surface in position 2, is symmetrical around the axis O the result will be that the PSD detector will produce a signal deviation that corresponds to the spot being represented a little closer to A' than right on point B'. This is due to the fact that the PSD detector produces a signal that corresponds to the position of the "light gravity centre". As the same number of photons (the spot was indeed symmetrical around the axis O) are dispersed over a longer distance in the direction of A' than the photons that are dispersed in the direction of C', so the of the "light gravity centre" position is shifted a little in direction of A'. Observe that the of the "light gravity centre" shift towards A' takes place despite the light spot being symmetrical around the axis O and independently of any possible image fault in the main lens.

The aforementioned shift of the of the "light gravity centre" position towards A' can, however, be minimised if the light spot, which the collimated beam gives rise to when it strikes the measurement surface, is made as small as possible. The reader can now better understand why we dedicated sections 4 to 8 of the PSD school to learning how to minimise the light spot's diameter on the measurement surface as much as possible. One of the reasons is that we thereby minimise the of the "light gravity centre" shift towards A' in figure 1.

The small residual error that, despite everything, remains can be measured and placed in a linearisation table. When the PSD detector emits a measurement signal - indicating the position of the light spot image on the PSD detector - to the computer that evaluates the signal and converts it into distance from the measured surface to the triangulation probe, it is then easy to compensate for such small residual errors.

We have now seen how we can reduce the of the "light gravity centre" shift towards A' by ensuring that the light spot diameter on the measurement surface is as small as possible. But we have still not taken account of possible image faults in the main lens.

There is a very good tool for investigating how the image on the PSD detector appears when the light spot is reproduced with the aid of the main lens and this is called a

spot diagram. In order to be able to calculate a spot diagram it is essential to use a computer containing an optical calculation program that, inter alia, can calculate spot diagrams. The computer then calculates the exact position of the light beams - that emanate from one of the points of the object plane of the lens selected by the operator - strikes the image plane. The number of light beams (from tens to several thousands) selected by the operator are distributed evenly across the aperture of the lens. The result is obtained either in the form of a diagram that, for example, with the aid of small crosses showing where the light beams strike the image plane, or in the form of a co-

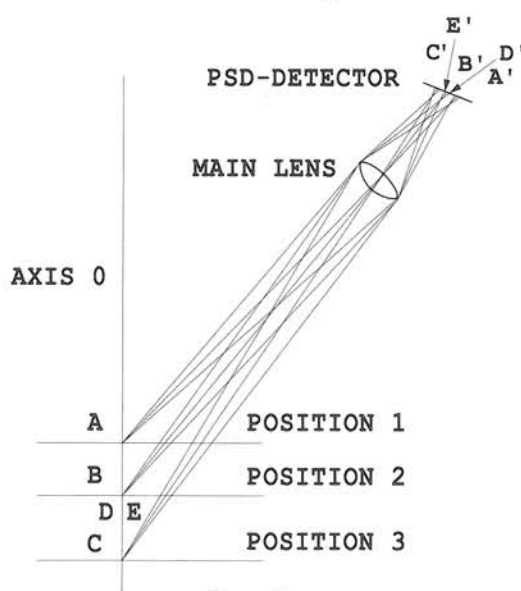


Figure 1

ordinate table that provides the x and y co-ordinates for where the light beams strike the image plane. The diagram provides an immediate, qualitative and visual experience on the capacity of the optics in question to give rise to a sharp image while it is necessary to use the co-ordinate table if one wishes to quantify the performance of the lens. Frequently, the calculation programs for optical spot diagrams also show the co-ordinates of the origin of the beams in the object plane as well as showing the co-ordinates of the spot centre

in the image plane. The spot's centre in the image plane can thereby be shown at least according to two different methods. Either one shows the co-ordinates for the point where the so-called chief ray cuts the image plane¹ (see figure 2), or also the computer calculates the average value for all x- and y-coordinates in the aforementioned table. This average value

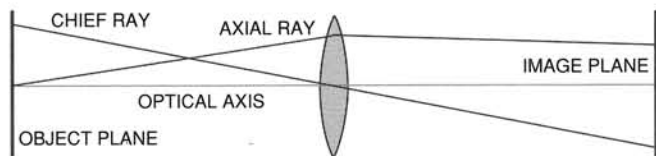


Figure 2.

corresponds to just that of the "light gravity centre" that the PSD detector indicates the position of. In addition, the computer also calculates the radius of the spot and indicates the spot radius in μm . It is also possible to obtain a very good idea as to how - in linear terms - different optical systems represent the spot's position on the PSD detector when the distance of the measurement surface from the triangulation probe is altered. To begin with we should therefore study some different spot diagrams for a main lens unit that only comprises a single lens.

Figure 3a shows a so-called spot diagram where the object plane and the image plane are at right angles to the optical axis and the light beams start from the point where the optical axis cuts the object plane. All other parameters agree with what is indicated in section 3 ($DE = 156,649$, $EF = 42,613$ and $f_E = 32,81$). Figure 3b shows the spot diagram obtained when the object plane and the image plane form the angles that are calculated in section 3 of the PSD

school, namely $\alpha=40^\circ$ and $\gamma=72,038^\circ$. It does not matter that $\alpha=40^\circ$ since the light beams that generate the spot diagram issue from a point on the optical axis without any difference between the spot diagram in figure 3a and 3b is due to the image plane forming the angle $\gamma=72,038^\circ$ towards the optical axis instead of 90° . If we compare the spot diagram in figure 3a with the spot diagram in figure 3b it is hard to see any difference with the naked eye. Nevertheless, according to the computer the focal point of the light spot is moved to $2\mu\text{m}$ in the direction of A' on figure 1. This fault is so small that it is easy to compensate for this when the triangulation probe is linearised.

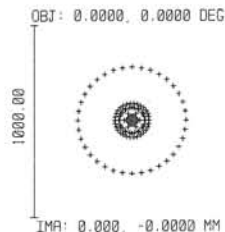


Figure 3a.

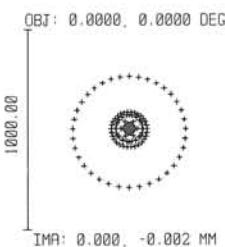


Figure 3b.

Let us now see what happens when the measurement surface is in position 1, ie. at point A on figure 1. Figure 4a shows the spot diagram when the chief ray is used as a reference and figure 4b shows the spot diagram when the centroid - the of the "light gravity centre" - is reference. As appears from figure 4a and 4b there is no difference between the spot diagrams themselves (after all it is exactly the same spot diagram as opposed to figures 3a and 3b where the image plane in the case of 3a was perpendicular to the optical axis and - in the case of 3b - formed the angle $72,038^\circ$ against the optical axis) but we can, from the deformed appearance, suspect that the of the "light gravity centre" does not coincide with the chief ray's intersection point with the image plane. The calculations also show that the of the "light gravity centre" is at a distance of 4,342 mm from the optical axis whereas the intersection point of the main beam is at a distance of 4,246 mm. The difference is $96\mu\text{m}$. Observe that this difference is only due to aberrations in the lens since all the light beams that are calculated in the spot diagram were emitted from the same point in the object plane. The computer shows that the spot radius is $642\mu\text{m}$. ie. the spot's greatest length is 1,284 mm. This is not a performance

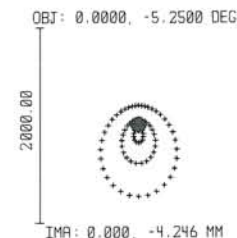


Figure 4a.

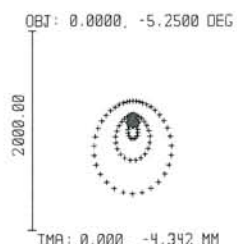


Figure 4b

that impresses and if, in addition, we were to take into consideration that the spot in reality is not point-shaped then the result will be even worse. There are maybe readers that believe that it is wholly in order to eliminate these faults in connection with the calibration of the triangulation probe but I do not agree with it. If the faults are large ones and are changed rapidly then the pre-calibrated triangulation probes become extremely sensitive for even small shifts of the parts involved.

We shall therefore - in the next section - study different lens types that do not introduce such large linear deviations as a single biconvex lens.

¹ A chief ray goes from a point in the object plane through the intersection point between the system's optical axis and the system's so-called aperture diaphragm. The aperture diaphragm limits the diameter of a beam that is parallel with the system's optical axis. An axial ray is a light ray that derives from the intersection point between the system's optical axis and the object



Published by
SiTek Electro Optics, Ögärdesvägen 13A,
SE-433 30 Partille, SWEDEN.
Phone: +46-31-340 03 30. Fax: +46-31-340 03 40.
Website: www.sitek.se
E-mail: info@sitek.se

SiTek[®]
ELECTRO OPTICS